EXTRACTION OF TYPHOON-DAMAGED FORESTS FROM MULTI-TEMPORAL HIGH-RESOLUTION POLARIMETRIC SAR IMAGES

Haipeng Wang[1], *Member, IEEE,* Kazuo Ouchi[2] , *Senior Member, IEEE* and Ya-Qiu Jin[1] , *Fellow, IEEE*

1. Key Laboratory of Wave Scattering and Remote Sensing Information (MoE), Fudan University, Shanghai 200433, China.
2. Department of Information Science, National Defense Academy, 1-10-20, Hashirimizu, Yokosuka 239-8686, Japan.

1. INTRODUCTION

The purpose of this study is to extract information on the forests destroyed by typhoons and to quantitatively estimate the damage levels by using multi-temporal high-resolution polarimetric synthetic aperture radar (SAR) data. The study area is located in Tomakomai, Hokkaido, Japan, where the area was used as a test site for estimating tree biomass by texture analyses [1]-[4]. The typhoon "Songda" (Japanese typhoon number 18) attacked the area in September 8th, 2004 and caused heavy damage over 50% in many stands. The forests map showing damaged stands from ground survey is available for comparison [5]. In the present study, we used two sets of SAR images acquired by the L-band fully polarimetric airborne Pi-SAR (Polarimetric Interferometric SAR) with 3m × 3m resolution (4-look in azimuth direction) [6]. The two sets of data were acquired before the typhoon damage in November 7th, 2002 (scene number L6407), and after the damage in November, 3rd, 2004 (scene number L8104), under similar conditions, such as the look direction and incidence angle (difference < 0.5° at the study area). The analyses and the results are summarized as follows.

2. ANALYSES AND RESULTS

Two methods were used to extracted damaged areas: the first is by simple subtraction of amplitude images, and the second is by subtraction of single-, double, and volume scattering components computed by the three-component scattering decomposition analysis [7].

Fig.1 shows the color composite images of L6407 and L8104 data. The red, green, and blue colors correspond respectively to the HH-, HV-, and VV-polarization images. Fig.2 is the ground-survey damage map made by the Hokkaido (Iburi-Tobu Branch) Forest Management, where the sites with red, yellow, and white colors correspond respectively to the stands damaged over 50%, those less than 50%, and 0%. It should be noted that the survey was made subjectively by averaging over each stand, but no details were given to the local damage within a stand. At the time of data acquisition (L8140) by Pi-SAR, fallen and half-fallen trees were still left in the stands, and they are classified as "damaged" stands. As will be seen in the followings, these fallen and half-fallen trees caused substantial discrepancy between the Pi-SAR data and ground-survey data.

Amplitude images were first analyzed by subtracting L8104 (after the typhoon) from L6407 (before the typhoon). RCS (Radar Cross Section) averaged over the whole image after the typhoon damage changed by -0.94 dB, 0.1 dB, and 1.28 dB at HH-, HV-, and VV-polarization data respectively in comparison with those before the damage as shown in Table 1. Note that for RCS in dB unit the amplitude values need to be doubled in the table. The same subtraction was made for the surface, double-bounce, and volume scattering power components computed by the three-component decomposition analysis [7] as shown in the three right columns in Table 1. It can be seen from the Table 1 that on a whole there is little difference in amplitude data. Some but not much increase in HH-polarization difference and decrease in VV-polarization difference are regarded as increase in

horizontally fallen trees and decrease in standing trees. Very little change is observed in HV-polarization data, indicating small change in multiple backscattering. In the decomposed power differences, the surface scattering (Ps) decreased by 20.28 dB because of decrease flat surface by fallen trees; while double-bounce scattering power (Pd) increased by 27.54 dB due to the increase in double reflection between ground and increase number of horizontal tree trunks. The volume scattering (Pv) showed small decrease by 0.20 dB as for the HV-poarization amplitude change.

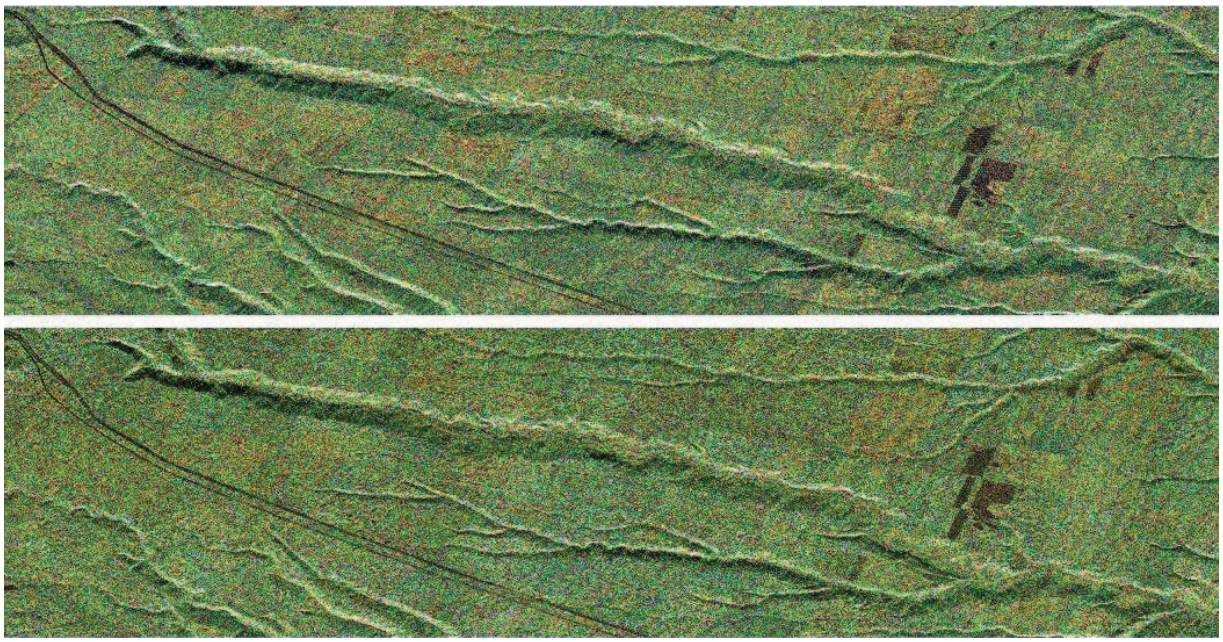

Fig. 1 Pi-SAR polarimetric image L6407 of the test site acquired in November 7th 2002 (top), and L8104 in November, 3rd, 2004 (bottom). Bottom: The red, green, and blue colors correspond respectively to HH-, HV-, and VV-polarization images.

Fig.2 Classified ground-survey map, where the stands with red and yellow colors correspond respectively to those with damage more than 50% and less than 50% but greater than 30%.

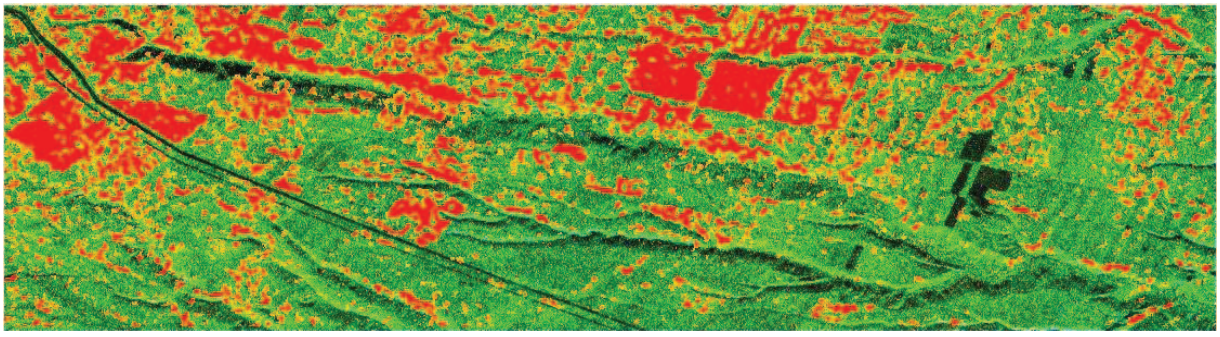

Fig. 3 Classified damage map based on amplitude subtraction of L8104 from L6407.

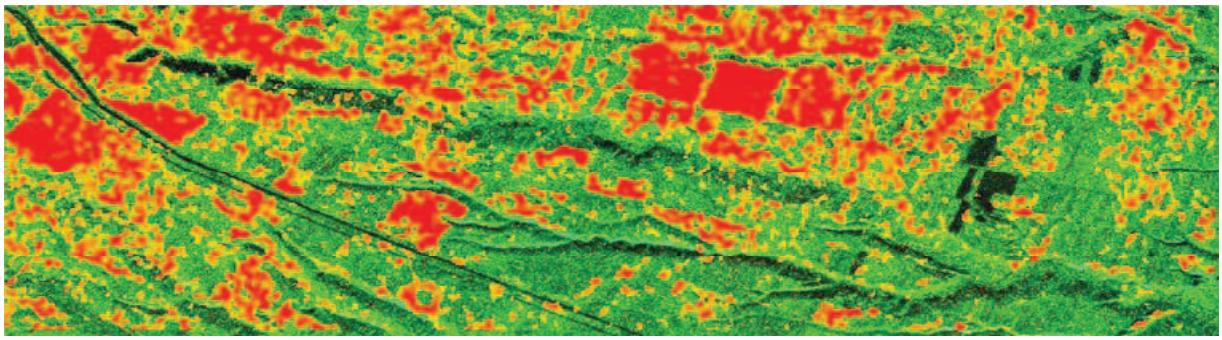

Fig. 4 Classified damage map based on subtraction of 3-component decomposition data of L8104 from L6407.

Table 1 Average amplitude of the entire scene before (L6407), after (L8104), and the difference (L6407-L8140) for different polarization data and different polarimetric power decomposition data (Ps: surface, Pd: double-bounce, Pv: volume scattering). The HH/HV/VV data are in amplitude unit and for power unit [dB].

scene number	HH	HV	VV	Ps	Pd	Pv
L6407	67.11	64.40	66.15	63.48	102.02	138.25
L8104	66.64	64.45	66.79	83.76	74.49	138.45
L6407-L8140	0.47	-0.05	-0.64	-20.28	27.54	-0.20

Table 2 Differences (L6407-L8140) in average amplitude for individual stands, and in polarimetric power decomposition data. The asterisk indicates the stands with less than 30% damage.

stand number	HH	HV	VV	Ps	Pd	Pv
196	0.84	0.60	-0.29	-22.16	14.12	1.13
197	0.95	0.58	-0.28	-39.47	38.28	1.09
198	0.87	0.33	-0.54	-32.94	39.19	0.48
217&218	0.86	0.44	-0.22	-32.17	35.43	0.77
243	0.90	0.45	-0.24	-34.08	37.59	0.78
245*	0.98	0.30	-0.28	-25.90	37.69	0.45
267	0.99	0.49	-0.06	-32.45	37.19	0.94
271	0.90	0.44	-0.51	-27.43	28.25	0.88
300	0.83	0.48	-0.01	-31.19	31.79	0.87
302*	0.79	0.32	-0.23	-27.34	35.59	0.44

Table 2 shows the differences in amplitude data and decomposed three-component data for individual stands. The most of stands show increase in HH-polarization data due mainly to backscattering from fallen trees, and decrease in VV-polarization data because of loss of standing (vertical) trees. The differences are larger than those of the average entire seen, because the stands with certain amount of difference were selected for Table 2. In the decomposed power differences in the right three columns of Table 2, The general trend is the roughly the same as

that of Table 1, although the values in subtraction increased because of the selected stands, i.e., Ps decreased and Pd increased after the typhoon due to the fallen trees, with small change in Pv. In order to interpret the results in depth, further experimental and theoretical studies are required. We are currently planning experiments in an anechoic chamber to determine the backscattering mechanisms from standing, half-fallen, and fallen-trees.

Estimated damaged stands based on amplitude and decomposition bases are shown in Figs. 3 and 4 respectively. From the comparison with the ground survey data, the accuracies of 64.1% and 77.7% were obtained for amplitude and decomposition data respectively. Thus, the experimental results do not appear in very good agreement with those observed from ground. There could be two reasons for this discrepancy. The first is that the ground-observation is subjective and does not specify damage areas within each stand, so that the ground-observation map shows "average damage" of each stand. The second is that fallen trees were still there when Pi-SAR observation was made. Half-fallen trees can be regarded as equivalent to standing trees by Pi-SAR, and they were categorized as fallen trees by ground-observation. Nevertheless, Pi-SAR has finer spatial resolution than the ground-observation map, and therefore, its data have potential to estimate damaged areas of forests caused by typhoons, provided, of course, that the correct quantitative backscattering mechanisms from standing, half-fallen, and standing trees are understood.

ACKNOWLEDGEMENT

This project is supported in part by the National Science Foundation of China under Grants 40901201, 60971091, and in part by the Open Fund of State Key Laboratory of Satellite Ocean Environment Dynamics, under contract No.SOED0907, and by SRF for ROCS, SEM.

REFERENCES

[1] H.Wang and K.Ouchi, "Accuracy of the *K*-distribution regression model for forest biomass estimation by high-resolution polarimetric SAR: Comparison of model estimation and field data," *IEEE Trans. Geosci. Remote Sens.*, vol.46, no.4, pp. 1058-1064, 2008.

[2] H.Wang, K.Ouchi, M.Watanabe, M.Shimada, T.Tadono, A.Rosenqvist, S.A.Romshoo, M.Matsuoka, T.Moriyama, and S.Uratsuka, "In Search of the Statistical Properties of High-Resolution Polarimetric SAR Data for the Measurements of Forest Biomass beyond the RCS Saturation Limits," *IEEE Geosci. Remote Sens. lett.*, vo.3 no.4, pp.495-499, 2006.

[3] M. Watanabe, M. Shimada, A. Rosenqvist, T. Todono, M. Matsuoka, S. A. Romshoo, K. Ohita, R. Furuta, K. Nakamura, and T. Moriyama, "Forest structure dependency of the relation between L-band σ^0 and biophysical parameters," *IEEE Trans. Geosci. Remote Sens.*, vol. 44, no. 11, pp. 3154–3165, Nov. 2006.

[4] H. Wang and K. Ouchi, "The relation between the order parameter of K-distribution in high-resolution polarimetric SAR data and forest biomass," in *Proc. IGARSS*, Seoul, Korea, Jul. 2005, pp. 4339–4342.

[5] Private Communication with Iburi-Tobu Forest Management, 3-4-1 Hinode-cho, Shiraoi, Hokkaido, Japan.

[6] T. Kobayashi, T. Umehara, M. Satake, A. Nadai, S. Uratsuka, T. Manabe, H. Masuko, M. Shimada, H. Shinohara, H. Tozuka, and M. Miyawaki, "Airborne dual-frequency polarimetric and interferometric SAR," *IEICE Trans. Commun.*, vol. E83-B, no. 9, pp. 1945–1954, 2000.

[7] A. Freeman and S. L. Durden, "A three-component scattering model for polarimetric SAR data," *IEEE Trans. Geosci. Remote Sens.*, vol.36, no.3, pp.963-973, 1998.

[8] C. J. Oliver, S. Quegan *Understanding Synthetic Aperture Radar Images*. London, U.K.: Artech House, 1998.